communications earth & environment

Article

A Nature Portfolio journal

https://doi.org/10.1038/s43247-025-02568-8

Ocean deoxygenation linked to ancient mesopelagic fish decline

Sven Pallacks[1,2] ✉, Patrizia Ziveri[1,3], Helen A. Jannke[4], Chien-Hsiang Lin[5], Adam V. Subhas[6], Eric Galbraith[1,3,7], Stefanie Kaboth-Bahr[8], Oliver Friedrich[9], André Bahr[9], Andreas Koutsodendris[9], Jörg Pross[9] & Richard D. Norris[4]

Mesopelagic fish are integral to ocean food webs and play an important role in carbon transport through their vertical migration behavior. Ocean deoxygenation caused by anthropogenic warming is expected to pose severe threats to mesopelagic fauna by enhancing physical stress and changing predator-prey relationships. In agreement with this expectation, our fish otolith record in a Mediterranean sediment core shows near absence of mesopelagic species during Sapropel deposition between ~7 and ~10 thousand years ago, concurrent with high surface productivity and low oxygenation of mid-depth waters. Instead, the otolith record is dominated by fish species adapted to epipelagic habitats, including European anchovy (*Engraulis encrasicolus*) and silvery lightfish (*Maurolicus muelleri*). Subsequent reoxygenation starting ~7 thousand years ago is accompanied by a three-fold increase in total otolith abundance. The large majority of these are mesopelagic lanternfish (Myctophidae) that dominate the otolith assemblage from the middle-Holocene to the present. Our findings corroborate expectations that future expansion of midwater deoxygenation could severely deplete mesopelagic fish communities over the coming centuries, with major impacts on marine fisheries, marine conservation, ocean food web structure, carbon storage and other marine ecosystem services.

Ocean deoxygenation through the intensification, expansion, and shoaling of Oxygen Minimum Zones (OMZs) is thought to pose a serious threat to mesopelagic fish communities[1]. OMZs tend to occur at mid-depth, where oxygen concentration is at its lowest, limiting macrofaunal life[2–4]. Global expansion, intensification, and shoaling of OMZs have been documented over the last several decades related to anthropogenic climate change[5–8], and ocean models project further decline of oxygen levels during this century[5,9–11]. The vertically expanded OMZ of the future is expected to compress the vertical nighttime habitat of mesopelagic fish species, 75% of which are lanternfish[12], and to shift their daytime habitat into the lower edge of the euphotic zone (Fig. 1a, b) where they are exposed to visual predators[1,4,13,14].

A potential decline of mesopelagic fish under expanded ocean hypoxia would have major implications for ocean productivity. Global mesopelagic fish biomass estimates range from 2 to 20 Gt[15,16], which is one to two orders of magnitude higher than world fisheries and aquaculture production in 2020[17]. Due to their large biomass and vertical migrating behavior, they are important contributors to the marine carbon cycle[18,19]. However, the effects of OMZ expansion on mesopelagic communities are still under debate, as their biological response to the combined effects of deoxygenation and other environmental stressors appears to be complicated[20,21]. Apart from oxygen saturation, other parameters like ocean temperature[22–24] and primary productivity[15,18] also play an important role in mesopelagic fish dynamics, and how species and communities adapt to long-term environmental variability[25].

The Eastern Mediterranean Sea is an ideal study area to investigate fish community response to changing ocean oxygen levels, as oceanographic conditions have alternated between a well-oxygenated and a hypoxic water column throughout the last 13.5 million years[26]. Cyclic hypoxia has periodically amplified organic matter preservation in sediments on millennial

[1]Institute of Environmental Science and Technology (ICTA), Universitat Autònoma de Barcelona (UAB), Bellaterra, Barcelona, Spain. [2]Smithsonian Tropical Research Institute (STRI), Balboa, Republic of Panama. [3]Catalan Institution for Research and Advanced Studies (ICREA), Barcelona, Spain. [4]Marine Biology/Laboratory of Paleobiology/Geosciences Research Division, Scripps Institution of Oceanography, San Diego, CA, USA. [5]Biodiversity Research Center, Academia Sinica, Taipei, Taiwan. [6]Department of Marine Chemistry and Geochemistry, Woods Hole Oceanographic Institution, Woods Hole, MA, USA. [7]Department of Earth and Planetary Sciences, McGill University, Montreal, QC, Canada. [8]Institute of Geological Sciences, Freie Universität Berlin, Berlin, Germany. [9]Institute of Earth Sciences, Heidelberg University, Heidelberg, Germany. ✉e-mail: Pallacks.s@gmail.com

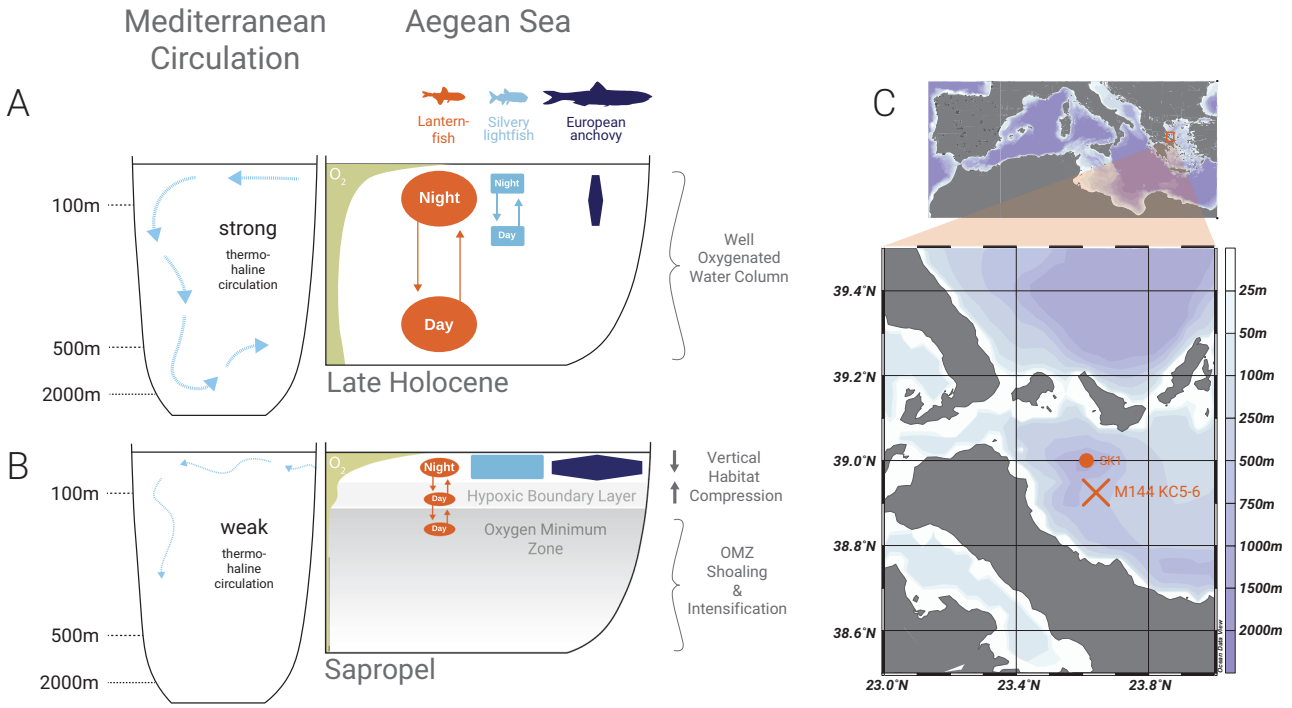

Fig. 1 | Ecological response of fish to changing oceanographic conditions during the Holocene in the central western Aegean Sea, adapted from previous studies[1,26,59]. **A** High mesopelagic fish production in a well-ventilated water column during the Late Holocene. **B** Enhanced/low epipelagic/mesopelagic fish production under expanded ocean hypoxia during Sapropel deposition. **C** Ocean data view bathymetry map[96] of study area and core locations of M144 KC5-6 (this study) and SK1[33,97].

timescales and caused the formation of dark, organic-rich sedimentary deposits, called sapropels, which are commonly interpreted as past analogs for future ocean deoxygenation under climate change[27] (Supplementary Note S2). Here we show that changes in ocean oxygen levels are associated with Holocene mesopelagic fish dynamics in the most recent of the sapropels (S1) by reconstructing fossil fish communities using ear bones (otoliths) in a sediment core from the central western Aegean Sea (see Methods; Supplementary Note S2). Total fish production is estimated by otolith accumulation rates (OAR). To evaluate fish community changes, we identified >84% of all otoliths at least to the family level.

Results and discussion

Eastern Mediterranean Holocene fish dynamics

We used otoliths to reconstruct fish dynamics throughout the last ~11.4 kyr in the central western Aegean (Figs. 1c, 2a, b; Supplementary Fig. S1; Supplementary Table S1). Prior to S1 deposition, species composition is dominated by the mesopelagic lanternfish family (Myctophidae; 32%) and silvery lightfish (*Maurolicus muelleri*; 40%). Epipelagic fish like the European anchovy (*Engraulis encrasicolus*) account for 9% of otolith flux. During sapropel deposition in the early Holocene between 9.9 and 7.0 kyr BP (Supplementary Table S2), the silvery lightfish (42%) still dominates the record, but the abundance of mesopelagic lanternfish declines by over half to 14%. Abundances of the European anchovy doubled to 18%. Otoliths from the Gadidae (5%) and Gonostomatidae (3%) families, both of which can be found living in meso- to bathypelagic depths, form minor parts of the sapropel fauna. Following sapropel S1, from ~7 kyr BP to present, lanternfish constitute 77% of the otolith assemblage, ranging between 71% and 91%. We identified a total of 12 lanternfish species (Supplementary Figs.S4 and S5) without substantial composition changes throughout the Middle to Late Holocene.

Ocean deoxygenation in the ancient Eastern Mediterranean Sea

The decline of lanternfish during the sapropel is in accord with hypotheses that mesopelagic species should do poorly as oxygen minima expand. Lanternfish habitat between 250 m and 600 m water depth[28] apparently became uninhabitable as the OMZ expanded. By comparison, the shallow habitats of the silvery lightfish (habitat depth: 80–225 m) and the European anchovy (habitat depth: 0–180 m) may have allowed both species to avoid the expansion of anoxic midwater conditions[28–30].

Numerical models and palaeoceanographic data on the distribution and intensity of the sapropel conditions have previously shown that hypoxic waters shoaled and oxygen depletion intensified in the early Holocene. During S1 formation, large parts of the Eastern Mediterranean Sea developed anoxic mid- to bottom waters[26,31,32], including the central western Aegean Sea[33,34]. Hypoxia is thought to have developed due to enhanced freshwater runoff and reduced evaporation in the eastern Mediterranean region[35,36]. The resulting intensified vertical stratification in surface waters impaired deep water formation and led to oxygen-depleted mid- to bottom waters[37]. Sapropel layers are rare in sediment cores recovered from water depths less than ~80 to ~125 m but are common below this depth[26,38] suggesting that the water column was severely anoxic below the wind-mixed surface ocean. The sporadic presence of otoliths (Supplementary Fig. S1) of the deep-water families Gonostomatidae and Gadidae suggests that the midwater environment, while hypoxic, never became fully euxinic (anoxic and charged with hydrogen sulfide (H_2S)), a condition lethal to most metazoans, including marine fish[39]. This is in line with previous studies reporting euxinic bottom water conditions only at considerably deeper sites compared to our study region[40–42].

The shallow OMZ and elevated riverine nutrient runoff are thought to have stimulated surface ocean productivity[26,32] in agreement with our finding that epipelagic European anchovy increased in abundance during the sapropel. There is comprehensive microfossil and geochemical proxy evidence from the Eastern Mediterranean Sea for large downward fluxes of organic matter to the seabed during S1 formation[43–48]. Planktic foraminiferal accumulation rates (Fig. 2f) also provide evidence for enhanced surface production at our study site during S1, as planktic foraminiferal standing stocks are positively related to primary production[49]. Furthermore, planktic foraminiferal species indicate highly productive surface conditions during

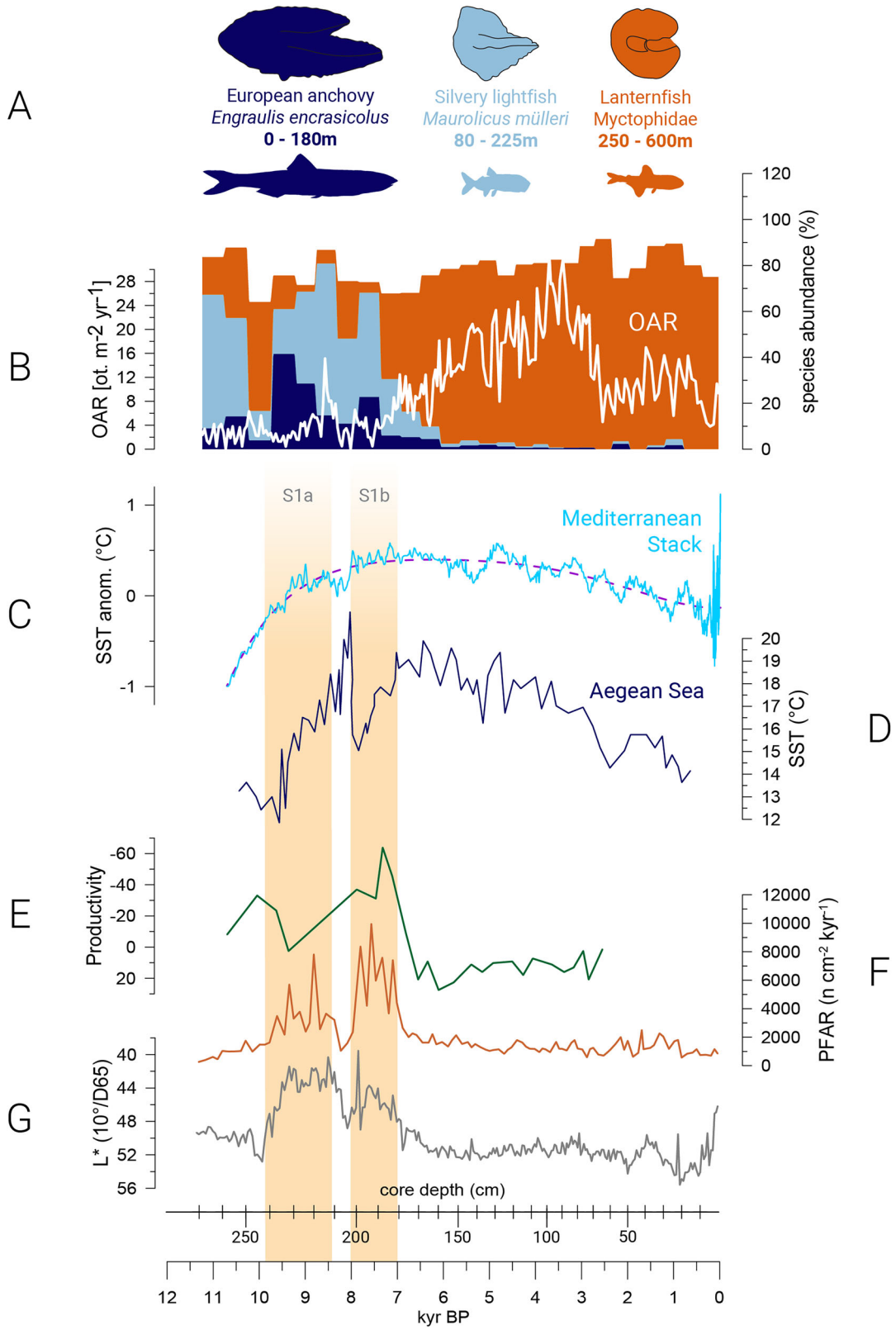

Fig. 2 | Paleo fish composition changes in the central western Aegean Sea throughout the last 11.4 kyr retrieved from a fossil otolith record (core: M144 KC5-6). A Sketches of most common fish species: European anchovy (Engraulis encrasicolus; dark blue), Silvery lightfish (Maurolicus mülleri; light blue); and the most common family: Lanternfish (Myctophidae; red) with habitat depth range indicated[28,30] (Supplementary Note S3). **B** Relative abundances of the three most common species/family as a cumulative stacked area plot of 10 cm bins. The white trend line shows total otolith accumulation rates (OAR_{tot}). **C** Stack of Sea Surface Temperature (SST) anomaly [°C] changes in the Mediterranean throughout the Holocene[76]. **D** SST [°C] variability and **E** productivity changes in the central west Aegean Sea (green line) shown by productivity proxies (upwelling and eutrophication; PCA3) from core SK-1 close to our study site[33]. **F** Planktic foraminiferal test accumulation rates (PFAR) and **G** sediment surface color scanning of core M144 KC5-6. Light brownish bands represent Sapropel S1a and S1b.

S1 close to our core location[33]. Hence, the decline in abundance of mesopelagic species during Sapropel S1 occurred against a background of generally higher organic matter production and increased surface ocean biological production.

Low mesopelagic fish production beneath a highly productive surface ocean

We attribute the near disappearance of lanternfish in the sapropel to their sensitivity to mid-depth oxygen concentrations linked to their vertical migration behavior (Figs. 1a, b, 2b; Supplementary Fig. S1e). While lanternfish have many vertical migration patterns, most species of lanternfish feed at epipelagic depths during the night and hide in dark, often oxygen-deprived mesopelagic waters during the day[50], as morphological and physical adaptations allow mesopelagic fish to inhabit low oxygen environments[51–53]. Consistent with this tolerance of low oxygen concentrations, warm water lanternfish species have been found increasing in abundance regardless of declining oxygen concentrations[54], and fish scale records from Peru show that mesopelagic fish can be abundant during periods associated with a well-developed, strong and shallow OMZ[24,55].

Yet even though mesopelagic fish can thrive in moderately hypoxic conditions, physiological adaptations of lanternfish to low oxygen conditions seem to be species specific[51], and depend on their development stage[56]. Studies in the OMZs of the Arabian Sea have shown avoidance of anoxic waters by several lanternfish species[57,58]. In the Eastern Tropical North Pacific, most lanternfish avoid the lowest oxygen concentrations (<1.8 µM O2) within the OMZ core, preferentially residing during daytime at slightly elevated oxygen levels in the Upper Oxycline (<10 µM O2)[56]. As oxygen falls to extremely low concentrations (no or very little dissolved oxygen) at mid-depth, lanternfish may have to transit through uninhabitable (anoxic) environments to reach their daytime depth horizons, with negative physiological impacts[3,59]. In the California Current, declining oxygen concentrations and OMZ expansion have been associated with a decrease in lanternfish abundance, with vertically migrating fish being particularly vulnerable to nighttime habitat compression[1]. In severely oxygen depleted ocean environments like the Black Sea, where highly anoxic mid- to bottom waters sit below a thin oxygenated surface layer, the mesopelagic fish community is apparently entirely absent[60,61]. Quantifying oxygen concentrations during sapropel formation in the Eastern Mediterranean is challenging as no direct nor proxy measurements from that period are provided. However, we hypothesize that during sapropel deposition oxygen conditions in the Aegean Sea were comparable to those in the modern Black Sea[62]. Accordingly, the OMZ was particularly strong (<1 µM O_2), extending from the seabed to about several tens of meters below the sea surface. Therefore, mesopelagic fish were unable to avoid oxygen stress by sheltering below the OMZ.

Mesopelagic fish migrate vertically by hundreds of meters within the water column[12], but the nature of this migration varies between different marine regions[63–66]. In our Aegean site, the extensive distribution of hypoxia likely forced mesopelagic fish into shallower habitat depths during daytime. A more surface-oriented lifestyle would have caused several ecological challenges related to competition and niche occupancy, such as increased predation risk due to enhanced visibility, reduced resource availability, and exposure to greater temperature variability and UV radiation, potentially exceeding their physiological limits[67,68] and leading to higher mortality rates (see Supplementary Note S4). Although to a lesser extent, mesopelagic fish may have shown some horizontal diel migration and potentially taken refuge in deeper areas of the wider central and north Aegean area[69]. However, we consider this unlikely, not only due to the given widespread occurrence of anoxic conditions across much of the Eastern Mediterranean Sea[26], but also because the distances involved would likely exceed the spatial scale of typical diel horizontal migrations, implying a more permanent habitat shift rather than a feasible daily movement. To conclude, either a shift towards shallower daytime habitat depths or permanent displacement, both triggered by an intensification and expansion of the OMZ, are in agreement with our finding that lanternfish are rare in the sapropel.

The surface ocean continued to be well oxygenated during sapropel deposition, as reflected by the fish community. For example, silvery lightfish dominate the fish assemblage during S1 deposition (Fig. 2b and Supplementary Fig. S1d), which we attribute to their ability to exploit highly productive near-surface habitats above the OMZ. In the Atlantic, silvery lightfish are associated with high chlorophyll-a values at the ocean surface[70], and in the Gulf of Corinth (Eastern Mediterranean), the species inhabits epipelagic daytime habitats at approximately 200 to 150 m water depth[28]. To better cope with enhanced predator pressure, the species is known for changing from diel vertical migration to schooling behavior at the surface, as reported at northern high latitudes when exposed to illuminated summer nights[29]. High epipelagic fish production during the sapropel is also indicated by the increase in abundance of European anchovy (Fig. 2b and Supplementary Fig. S1c). These fish thrive in oceanic systems characterized by strong, shallow OMZs and high surface productivity, as reported from the modern Black Sea[71] and from paleorecords and fishery datasets off the coast of Peru[55,72]. Furthermore, the northern Aegean Sea provides one of three major European anchovy stocks in the Mediterranean[73]. Cooler, fresher, and zooplankton-rich surface waters during Sapropel formation likely provided superior spawning conditions for adults, promoting larger anchovy stocks in the Aegean Sea[69,74]. However, these advantages would have been offset if higher mortality rates occurred due to inter- or intraspecific competition, cannibalism, or increased predation by other zooplanktivores. Increasing sea surface temperatures (SST) throughout sapropel formation might explain lower anchovy OAR in S1b compared to S1a (Fig. 2b–d), as ocean warming above their optimum temperature can have led to adverse effects on their growth and abundance[75]. In our record, enhanced abundances of European anchovy and silvery lightfish are consistent with increased surface ocean primary productivity, indicated by elevated planktic foraminifera production (Fig. 2f). Whatever the process, both species were apparently less susceptible to an intensification and shoaling of the OMZ during S1 deposition than lanternfish, while still benefiting from enhanced productivity at the surface.

Mid-to-Late Holocene recovery of the mesopelagic fish assemblage

Total mean Otolith Accumulation Rates (OAR_{tot}) describe great variations of total fish abundance throughout the last ~11.4 kyr, likely driven by shifting environmental conditions in the Eastern Mediterranean basin[26,33,76,77]. In the early Holocene, OAR_{tot} is low (2.7 otoliths m^{-2} yr^{-1}) and only increases slightly to 4.3 otoliths m^{-2} yr^{-1} in the sapropel. Following the sapropel, after 7 kyr BP, the OAR_{tot} increases by ~3x over sapropel otolith production to 14.1 otoliths m^{-2} yr^{-1}, mainly driven through changes in lanternfish abundance as indicated by a 20-fold increase by myctophid Otolith Accumulation Rates (OAR_{myc}). In the late Holocene, OAR_{tot} reaches a peak of 32.4 otoliths m^{-2} yr^{-1} at 3.7 kyr BP before falling to an average of 10.1 otoliths m^{-2} yr^{-1} during the last 2.5 kyr.

We attribute these trends in OAR_{tot} to a combination of variables that reflect the major drivers of fish abundance in the mesopelagic environment. Lanternfish population dynamics are known to respond to variations in oxygenation, habitat temperature, and productivity[15,18,22,24,25,54,64]. The high relative abundances of lanternfish prior to S1a can be attributed to the low OAR of all species, >10 kyr ago, which is consistent with both low productivity and cold temperatures in the early Holocene. De-oxygenation between 7–10 kyr suppressed overall fish productivity, as indicated by the OAR_{tot} values, but epipelagic species did comparatively better than mesopelagic fish, as noted above. When the Mediterranean became reoxygenated again about 7 kyr ago, mesopelagic production boomed, perhaps because high growth rates in the warm ocean offset the drop in surface ocean productivity. Sea surface temperatures fell in the Aegean in the past 3.5 kyr BP, and this drop in temperature may account for the overall decline in OAR_{tot}. Our findings are consistent with former studies that found enhanced mesopelagic fish production under warmer conditions[22,23] over the interval in which there were no dramatic changes in oxygenation.

However, variations within the overall composition of the mesopelagic fish community during the mid- to late Holocene could not be clearly attributed to changes in SST, which contrasts previous findings that report higher relative abundances of lanternfish during warm interglacial periods compared to colder glacial intervals[78]. Given that the relationship between lanternfish abundance and SST is complex and still insufficiently understood, combined with the limited availability of high-resolution environmental data for the late Holocene in our study area, we can only hypothesize that temperature might be important for lanternfish population dynamics in our record. In general, our finding that lanternfish are abundant outside the sapropel interval agrees well with the typical dominance of lanternfish in modern assemblages. For example, the otoliths of lanternfish dominate over other fish groups in surface sediments from the Western Atlantic[79], the Eastern Atlantic[80], the Eastern Pacific[25], the Red Sea[81],and the Mediterranean Sea[82,83]. Fish catch data and acoustic backscatter analysis[15,84] also corroborate the dominance of lanternfish in the modern ocean in terms of biomass and species diversity[12]. Furthermore, the lanternfish species composition in our record is similar to recent fossil assemblages[83] and modern fish catches[28,85] from the Mediterranean Sea, in agreement with our findings.

Informing the mesopelagic fish response to future ocean deoxygenation through the fossil otolith record

In the future, models suggest that OMZs will intensify and expand, shifting the upper hypoxic boundary layer closer towards the sea surface[5,10,11]. Deoxygenation is expected to affect the vertical habitat depth range for mesopelagic species since this is strongly influenced by oxygen concentrations[13,14,56,86]. Shoaling of daytime habitat and vertical compression of nighttime habitat have been hypothesized to alter predator-prey relationships with negative impacts on the mesopelagic fish community[1,3,59]. Our paleo data are broadly in agreement with these expectations, showing low total otolith abundances and near absence of mesopelagic fish during sapropel formation driven by low abundance rather than preservation effects (Text S4). The positive relation between lanternfish abundance and SST in the younger Holocene record is consistent with enhanced mesopelagic fish productivity in warmer waters under some conditions[22,23,54]. Nonetheless, despite ocean warming and high surface productivity during S1 formation, the near absence of lanternfish indicates habitat compression during S1 and highlights the potentially dramatic importance of very low oxygen levels for the mesopelagic fish community, overriding the effects of ocean warming and productivity changes.

Downcore otolith studies that reconstruct fish dynamics are extremely rare yet critically important for understanding how ecological key groups, such as lanternfish, are affected by climate change and ocean deoxygenation. Despite their inherent limitations in temporal and spatial resolution, the strength of paleoecological studies lies in their ability to capture ecological responses over long timescales, ranging from hundreds to thousands of years. Therefore, extending the collection and analysis of otolith records is essential to capture broader regional patterns and account for spatial variability in fish communities. Future research could explore stable isotope and trace element analyses, as well as morphometric studies throughout high-resolution otolith records, to infer environmental changes and life stage transitions across periods of extreme climatic variability. Such efforts would provide valuable insights into the responses of these important fish groups to past climate events, offering crucial perspectives on their resilience and adaptability in the face of future climate change.

Materials and methods

Material

The study is based on Core M144 KC 5-6, collected with a Kasten Corer system (appendix in ref. 87.) at 559.2 m water depth in the central western Aegean Sea (38°55.545'N; 23°38.684'E) during cruise M144 from December 2017 to January 2018 on board R/V Meteor[88]. Sapropel phases are identified as dark shaded bands (Supplementary Note S5; Supplementary Fig. S2, Supplementary Table S2), and their boundaries are well defined based on Br content[89]. The 345 cm long, 30 ×30 cm Kasten Core was subsampled into cores A and B, each core representing the top 272 cm and a surface area of 14.5 × 14.5 cm, sliced every 1 cm. The 0.5 cm thick walls of the Plexiglas boxes used for subsampling result in three missing samples at depths 100.5 cm, 101.5 cm, and 202 cm. We obtain bulk sediment mass after drying each 1 cm slice at 50–60 °C for approximately three weeks until samples reach constant dry weight. Dry samples are washed over a 125 µm screen, before drying them at 50–60 °C for about 24 h. Dry bulk density for each sample is calculated by dividing dry bulk sediment mass by sample volume.

Age model

Eleven radiocarbon dates (^{14}C) are obtained from different depths (Supplementary Table S3) spanning the entire core length, measured in planktic foraminifera (*Globigerinoides ruber* white) tests, isolated from the 250 to 315 µm fraction. Analysis is performed by using accelerator mass spectrometry (AMS) at the NOSAMS facility at Woods Hole Oceanographic Institution[90]. By using a globally averaged mixed-layer reservoir age of approximately 400 yr., the age depth model was constructed through Bayesian statistics, employing the R-code package rbacon (version 3.1.1) and the calibration curve Marine20 to convert ^{14}C dates to calendar ages[82,83]. Ages are reported with minimum and maximum 95% confidence ranges (Supplementary Fig. S3), and results are discussed in supplementary material (Supplementary Note S6).

Otoliths

After dry sieving over a > 250 µm screen, which is an appropriate mesh size to process otoliths[22,80,81,83], we isolate all otoliths and otolith fragments from the coarse size fraction and archive them on micropaleontological slides. Otolith count and identification are performed on both cores A and B, with lower resolution between 0.5 cm and 151.5 cm, and highest resolution between 152.5 cm and 272.5 cm. A binocular stereo microscope (magnification 10x–20x) and a bifurcated illuminator are used to undertake counting and taxonomic analysis.

Otolith accumulation rates (OAR, otoliths m^{-2} yr^{-1}) are estimated by dividing raw otolith counts by dry bulk sediment mass (g^{-1}), then multiplying by the sediment accumulation rate (cm yr^{-1}), dry bulk density (g cm^{-3}) of each sample, and multiplying by ten.

Identification of otoliths to the lowest taxonomic level is based on an automatic taxon identification software[91], web database[92], and otolith catalogs from the Mediterranean region[80,93]. We classified a total number of 3272 otoliths into one of six groups: the families Myctophidae (68.0%), Sternoptychidae (9.6%), Engraulidae (3.6%), Gadidae (1.8%), and Gonostomatidae (1.5%), representing the most common taxa of the otolith record, and Other (15.5%). Within the five families, the following species are identified: Myctophidae: *Benthosema glaciale*, *Ceratoscopelus maderensis*, *Diaphus holti*, *Electrona risso*, *Hygophum benoiti*, *Hygophum hygomii*, *Lampanyctus crocodilus, Lampanyctus pusillus*, *Lobianchia dofleini*, *Myctophum punctatum*, *Notoscopelus elongatus*, *Symbolophorus veranyi*; Sternoptychidae: *Argyropelecus hemigymnus*, *Maurolicus muelleri*; Engraulidae: *Engraulis encrasicolus*; Gadidae: *Gadiculus argenteus*, *Micromesistius poutassou*. Most of the counted myctophids are small juveniles, which is in line with other paleo studies (e.g. planktic foraminifers) and reflects the living myctophid assemblage, as the majority caught by trawling are larvae and/or juveniles[12]. Owing to the selected size fraction (>250 µm), we do not find any otoliths belonging to larval stages in the assemblage. Even though larval specimens are present in the 125–250 µm fraction, we have excluded this dataset from the study due to the taxonomic identification uncertainties associated with otoliths of this size range. Overall, otolith preservation is good throughout the entire core, and since otoliths are deposited in the same sediment, undergoing the same potential taphonomic processes[94], we do not expect any preservation control on otolith numbers in the sediments before, during, and after sapropel formation (Supplementary Note S4). Otoliths we cannot identify due to deficient preservation and/or a missing modern analog, we classify as unidentified. Unidentified and identified otoliths not belonging to one of the target families are grouped into Other (Supplementary Fig. S1). The 15.5% of specimens categorized as 'Other' are

consistent with proportions reported in previous studies[22,25] and are not expected to significantly influence our findings. Furthermore, the predominance of the target families—Myctophidae, Engraulidae, and Sternoptychidae—comprising over 81% of the fossil assemblage, provides a robust dataset for analyzing their population dynamics. Color images for each target species are taken with reflected light and a black background using a Canon EOS 650 D camera device attached to a Leica Z16 AP0 at UAB laboratory facilities, to produce a reference catalog (Supplementary Figs. S4–6) and to perform automated taxon identification through the AFORO software[91].

Relative abundance and OAR records for the six groups are smoothed by calculating the mean values for 10 cm bins (Supplementary Fig. S1). Mean values regarding sapropel phases are calculated for otolith relative abundance and otolith accumulation rate (OAR) for each target family (Supplementary Table S2).

Planktic foraminifera

For the calculation of planktic foraminiferal accumulation rates (PFAR), a total of 108 samples were taken from Core M144 KC5-6 in a sample resolution of 2–4 cm. All sediment samples were first dried and weighed, then disaggregated in distilled water and sieved through a 63 µm mesh. Planktic foraminiferal counts are based on the >125 µm size fraction. If the sample counted more than 250–300 specimens, representative splits of the sample material were counted. Planktic foraminiferal counts (PFAR) are then recalculated for the entire sample. PFAR were calculated following the equation (Eq. 1) from ref. 95:

$$\mathrm{PFAR} = \mathrm{F} * \mathrm{LSR} * \mathrm{DBS}\,[\mathrm{n\,cm^{-2}kyr^{-1}}] \quad (1)$$

where F represents the abundance of planktic foraminifera (n g^{-1}), LSR denotes the linear sedimentation rate (cm kyr^{-1}), and DBS refers to the dry bulk sediment (g cm^{-3}) (g = grams of dry sediment).

Color scanning

A MINOLTA CM-700d hand-held spectrophotometer was used, combined with a CM-A178 target mask (Ø 8 mm, with plate) to color scan M144 KC5-6 each cm downcore on board. The sediment surface was cleaned and covered air-bubble-free with a polyethylene foil before scanning. Color data were reported in the CIELAB space using the $L^*a^*b^*$ system. To calibrate the spectrophotometer, a Konica Minolta White Calibration Cap CM-A177 and a Zero Calibration Box CM-A182 were used. Spectral reflectance was measured over a wavelength spectrum from 400 to 700 nm. The L^* and a^* values were used to define sapropel phases (Fig. 2g).

Reporting summary

Further information on research design is available in the Nature Portfolio Reporting Summary linked to this article.

Data availability

All data generated or analyzed during this study are included in this published article (and its supplementary information files). All data is also publicly available online for download at PANGAEA Data Publisher (https://doi.pangaea.de/10.1594/PANGAEA.974530).

Received: 18 July 2024; Accepted: 9 July 2025;
Published online: 28 July 2025

References

1. Koslow, J. A., Goericke, R., Lara-Lopez, A. & Watson, W. Impact of declining intermediate-water oxygen on deepwater fishes in the California Current. *Mar. Ecol. Prog. Ser.* **436**, 207–218 (2011).
2. Gilly, W. F., Beman, J. M., Litvin, S. Y. & Robison, B. H. Oceanographic and biological effects of shoaling of the oxygen minimum zone. *Annu. Rev. Mar. Sci.* **5**, 393–420 (2013).
3. Wishner, K. F., Outram, D. M., Seibel, B. A., Daly, K. L. & Williams, R. L. Zooplankton in the eastern tropical north Pacific: Boundary effects of oxygen minimum zone expansion. *Deep Sea Res. Part I Oceanogr. Res. Pap.* **79**, 122–140 (2013).
4. Seibel, B. A. & K. F. Wishner, K. F. in *Ocean Deoxygenation: Everyone's Problem*. (eds Laffoley. D. J. & Baxter. M.). chap. 8.1, 265–276. (IUCN, 2019).
5. Bindoff, N. L. et al. in *IPCC Special Report on the Ocean and Cryosphere in a Changing Climate*. (eds H.-O. Pörtner H.-O.) 447–587 (Cambridge, UK and New York, NY, USA, 2019).
6. Helm, K. P. & Bindoff, N. L. & Church, J. A. Observed decreases in oxygen content of the global ocean. *Geophys. Res. Lett.* **38**, L23602 (2011).
7. Schmidtko, S., Stramma, L. & Visbeck, M. Decline in global oceanic oxygen content during the past five decades. *Nature* **542**, 335–339 (2017).
8. Stramma, L., Johnson, G. C., Sprintall, J. & Mohrholz, V. Expanding oxygen-minimum zones in the tropical oceans. *Science* **320**, 655–658 (2008).
9. Kwiatkowski, L. et al. Twenty-first century ocean warming, acidification, deoxygenation, and upper-ocean nutrient and primary production decline from CMIP6 model projections. *Biogeosciences* **17**, 3439–3470 (2020).
10. Shaffer, G., Olsen, S. M. & Pedersen, J. O. P. Long-term ocean oxygen depletion in response to carbon dioxide emissions from fossil fuels. *Nat. Geosci.* **2**, 105–109 (2009).
11. Keeling, R. F., Körtzinger, A. & Gruber, N. Ocean deoxygenation in a warming world. *Annu. Rev. Mar. Sci.* **2**, 199–229 (2010).
12. Catul, V., Gauns, M. & Karuppasamy, P. K. A review on mesopelagic fishes belonging to family Myctophidae. *Rev. Fish. Biol. Fish.* **21**, 339–354 (2011).
13. Bianchi, D., Galbraith, E. D., Carozza, D. A., Mislan, K. A. S. & Stock, C. A. Intensification of open-ocean oxygen depletion by vertically migrating animals. *Nat. Geosci.* **6**, 545–548 (2013).
14. Netburn, A. N. & Koslow, J. A. Dissolved oxygen as a constraint on daytime deep scattering layer depth in the southern California current ecosystem. *Deep Sea Res. Part I Oceanogr. Res. Pap.* **104**, 149–158 (2015).
15. Irigoien, X. et al. Large mesopelagic fishes biomass and trophic efficiency in the open ocean. *Nat. Commun.* **5**, 3271 (2014).
16. Proud, R., Handegard, N. O., Kloser, R. J., Cox, M. J. & Brierley, A. S. From siphonophores to deep scattering layers: uncertainty ranges for the estimation of global mesopelagic fish biomass. *ICES J. Mar. Sci.* **76**, 718–733 (2019).
17. FAO. *The State of World Fisheries and Aquaculture 2022. Towards Blue Transformation* (FAO, Rome, Italy, 2022).
18. Davison, P. C., Checkley, D. M., Koslow, J. A. & Barlow, J. Carbon export mediated by mesopelagic fishes in the northeast Pacific Ocean. *Prog. Oceanogr.* **116**, 14–30 (2013).
19. Saba, G. K. et al. Toward a better understanding of fish-based contribution to ocean carbon flux. *Limnol. Oceanogr.* **66**, 1639–1664 (2021).
20. Claireaux, G. & Chabot, D in *Ocean Deoxygenation: Everyone's Problem* (eds. Laffoley, D. & Baxter, J. M.) chap. 8.11, 461–484 (IUCN, 2019).
21. Koslow, J. A. in *Ocean Deoxygenation: Everyone's Problem* (eds. Laffoley, D. & Baxter, J. M) chap. 8.4, 321–339 (IUCN, 2019).
22. Lin, C.-H., Wei, C.-L., Ho, S. L. & Lo, L. Ocean temperature drove changes in the mesopelagic fish community at the edge of the Pacific Warm Pool over the past 460,000 years. *Sci. Adv.* **9**, eadf0656 (2023).
23. Proud, R., Cox, M. J. & Brierley, A. S. Biogeography of the global ocean's mesopelagic zone. *Curr. Biol.* **27**, 113–119 (2017).
24. Salvatteci, R. et al. Smaller fish species in a warm and oxygen-poor Humboldt Current system. *Science* **375**, 101–104 (2022).

25. Jones, W. A. & Checkley, D. M. Mesopelagic fishes dominate otolith record of past two millennia in the Santa Barbara Basin. *Nat. Commun.* **10**, 4564 (2019).
26. Rohling, E. J., Marino, G. & Grant, K. Mediterranean climate and oceanography, and the periodic development of anoxic events (sapropels). *Earth-Sci. Rev.* **143**, 62–97 (2015).
27. Mancini, A. M. et al. The past to unravel the future: Deoxygenation events in the geological archive and the anthropocene oxygen crisis. *Earth-Sci. Rev.* **249**, 104664 (2024).
28. Kapelonis, Z. et al. Seasonal patterns in the mesopelagic fish community and associated deep scattering layers of an enclosed deep basin. *Sci. Rep.* **13**, 17890 (2023).
29. Kaartvedt, S., Knutsen, T. & Holst, J.-C. Schooling of the vertically migrating mesopelagic fish Maurolicus muelleri in light summer nights. *Mar. Ecol. Prog. Ser.* **170**, 287–290 (1998).
30. Giannoulaki, M. et al. Characterizing the potential habitat of European anchovy Engraulis encrasicolus in the Mediterranean Sea, at different life stages. *Fish. Oceanogr.* **22**, 69–89 (2013).
31. Rohling, E. J., Rijk, S. D., Myers, P. G. & Haines, K. Palaeoceanography and numerical modelling: the Mediterranean Sea at times of sapropel formation. *Geol. Soc. Lond. Spec. Publ.* **181**, 135–149 (2000).
32. Schmiedl, G. et al. Climatic forcing of eastern Mediterranean deep-water formation and benthic ecosystems during the past 22000 years. *Quat. Sci. Rev.* **29**, 3006–3020 (2010).
33. Kontakiotis, G. Late Quaternary paleoenvironmental reconstruction and paleoclimatic implications of the Aegean Sea (eastern Mediterranean) based on paleoceanographic indexes and stable isotopes. *Quat. Int.* **401**, 28–42 (2016).
34. Casford, J. S. L. et al. A stratigraphically controlled multiproxy chronostratigraphy for the eastern Mediterranean. *Paleoceanography* **22**, PA4215 (2007).
35. Rohling, E. J. & Hilgen, F. J. The eastern Mediterranean climate at times of sapropel formation: a review. *Geologie en. Mijnb.* **70**, 253–264 (1991).
36. Kallel, N. et al. Enhanced rainfall in the Mediterranean region during the last Sapropel Event. *Oceanol. Acta* **20**, 697–712 (1997).
37. Stratford, K., Williams, R. G. & Myers, P. G. Impact of the circulation on sapropel formation in the eastern Mediterranean. *Glob. Biogeochem. Cycles* **14**, 683–695 (2000).
38. Perissoratis, C. & Piper, D. J. W. Age, regional variation, and shallowest occurrence of S1 sapropel in the northern Aegean Sea. *Geo-Mar. Lett.* **12**, 49–53 (1992).
39. Meyer, K. M. & Kump, L. R. Oceanic Euxinia in Earth history: causes and consequences. *Annu. Rev. Earth Planet. Sci.* **36**, 251–288 (2008).
40. Andersen, M. B., Matthews, A., Bar-Matthews, M. & Vance, D. Rapid onset of ocean anoxia shown by high U and low Mo isotope compositions of sapropel S1. *Geochem. Perspect. Lett.* **15**, 10–14 (2020).
41. Azrieli-Tal, I. et al. Evidence from molybdenum and iron isotopes and molybdenum–uranium covariation for sulphidic bottom waters during Eastern Mediterranean sapropel S1 formation. *Earth Planet. Sci. Lett.* **393**, 231–242 (2014).
42. Slomp, C. P., Thomson, J. & de Lange, G. J. Controls on phosphorus regeneration and burial during formation of eastern Mediterranean sapropels. *Mar. Geol.* **203**, 141–159 (2004).
43. Castradori, D. Calcareous nannofossils and the origin of eastern Mediterranean sapropels. *Paleoceanography* **8**, 459–471 (1993).
44. Thomson, J. et al. Florisphaera profunda and the origin and diagenesis of carbonate phases in eastern Mediterranean sapropel units. *Paleoceanography* **19**, PA3003 (2004).
45. Incarbona, A., Abu-Zied, R. H., Rohling, E. J. & Ziveri, P. Reventilation episodes during the sapropel s1 deposition in the eastern Mediterranean based on holococcolith preservation. *Paleoceanogr. Paleoclimatol.* **34**, 1597–1609 (2019).
46. Higgins, M. B., Robinson, R. S., Carter, S. J. & Pearson, A. Evidence from chlorin nitrogen isotopes for alternating nutrient regimes in the Eastern Mediterranean Sea. *Earth Planet. Sci. Lett.* **290**, 102–107 (2010).
47. Filippidi, A. & De Lange, G. J. Eastern Mediterranean deep water formation during sapropel S1: a reconstruction using geochemical records along a bathymetric transect in the Adriatic outflow region. *Paleoceanogr. Paleoclimatol.* **34**, 409–429 (2019).
48. Sachs, J. P. & Repeta, D. J. Oligotrophy and nitrogen fixation during eastern Mediterranean sapropel events. *Science* **286**, 2485–2488 (1999).
49. Schiebel, R. & Hemleben, C. Modern planktic foraminifera. *Paläontologische Z.* **79**, 135–148 (2005).
50. Salvanes, A. G. V. & Kristoffersen, J. B. in *Encyclopedia of Ocean Sciences* (ed. Steele. J. H.) 1711–1717 (Academic Press, Oxford, 2001).
51. Lopes, A. R. et al. Oxidative stress in deep scattering layers: Heat shock response and antioxidant enzymes activities of myctophid fishes thriving in oxygen minimum zones. *Deep Sea Res. Part I: Oceanogr. Res. Pap.* **82**, 10–16 (2013).
52. Torres, J. J., Grigsby, M. D. & Clarke, M. E. Aerobic and anaerobic metabolism in oxygen minimum layer fishes: the role of alcohol dehydrogenase. *J. Exp. Biol.* **215**, 1905–1914 (2012).
53. Cornejo, R. & Koppelmann, R. Distribution patterns of mesopelagic fishes with special reference to Vinciguerria lucetia Garman 1899 (Phosichthyidae: Pisces) in the Humboldt Current Region off Peru. *Mar. Biol.* **149**, 1519–1537 (2006).
54. Koslow, J. A. et al. The evolving response of mesopelagic fishes to declining midwater oxygen concentrations in the southern and central California Current. *ICES J. Mar. Sci.* **76**, 626–638 (2019).
55. Salvatteci, R. et al. Fish debris in sediments from the last 25 kyr in the Humboldt current reveal the role of productivity and oxygen on small pelagic fishes. *Prog. Oceanogr.* **176**, 102114 (2019).
56. Maas, A. E., Frazar, S. L., Outram, D. M., Seibel, B. A. & Wishner, K. F. Fine-scale vertical distribution of macroplankton and micronekton in the Eastern Tropical North Pacific in association with an oxygen minimum zone. *J. Plankton Res.* **36**, 1557–1575 (2014).
57. Nafpaktitis, B. G. Systematics and distribution of lanternfishes of the genera Lobianchia and Diaphus (Myctophidae) in the Indian Ocean. *Nat. Hist. Mus. Los Angeles County Sci. Bull.* **30**, 1–92 (1978).
58. Nafpaktitis, B. G. & Nafpaktitis, M. *Lanternfishes (Family Myctophidae) collected during cruises 3 and 6 of the R/V Anton Bruun in the Indian Ocean*. (Los Angeles County Museum of Natural History, 1969).
59. Seibel, B. A. Critical oxygen levels and metabolic suppression in oceanic oxygen minimum zones. *J. Exp. Biol.* **214**, 326–336 (2011).
60. Ostrovskii, A. & Zatsepin, A. Short-term hydrophysical and biological variability over the northeastern Black Sea continental slope as inferred from multiparametric tethered profiler surveys. *Ocean Dyn.* **61**, 797–806 (2011).
61. Capet, A., Vandenbulcke, L., Veselka, M. & Grégoire, M. 3.6 Decline of the Black Sea oxygen inventory. *J. Operat. Oceanogr*. **11**, s103–s106 (2018).
62. Callieri, C. et al. The mesopelagic anoxic Black Sea as an unexpected habitat for Synechococcus challenges our understanding of global "deep red fluorescence. *ISME J.* **13**, 1676–1687 (2019).
63. Badcock, J. & Merrett, N. R. Midwater fishes in the eastern North Atlantic—I. Vertical distribution and associated biology in 30°N, 23°W, with developmental notes on certain myctophids. *Prog. Oceanogr.* **7**, 3–58 (1976).
64. Olivar, M. P. et al. Variation in mesopelagic fish community composition and structure between Mediterranean and Atlantic waters around the Iberian Peninsula. *Front. Marine Sci.* **9**, 1028717 (2022).
65. Olivar, M. P. et al. Vertical distribution, diversity and assemblages of mesopelagic fishes in the western Mediterranean. *Deep Sea Res. Part I: Oceanogr. Res. Pap.* **62**, 53–69 (2012).

66. Mytilineou, C. et al. Deep-water fish fauna in the Eastern Ionian Sea. *Belgian J. Zool.* **135**, 229 (2005).
67. Zagarese, H. E. & Williamson, C. E. The implications of solar UV radiation exposure for fish and fisheries. *Fish. Fish.* **2**, 250–260 (2001).
68. Andresen, H. et al. Mesopelagic fish traits: functions and trade-offs. *Fish. Fish.* **26**, 83–103 (2025).
69. Isari, S., Fragopoulu, N. & Somarakis, S. Interranual variability in horizontal patterns of larval fish assemblages in the northeastern Aegean Sea (eastern Mediterranean) during early summer. *Estuar. Coast. Shelf Sci.* **79**, 607–619 (2008).
70. Dove, S., Tiedemann, M. & Fock, H. O. Latitudinal transition of mesopelagic larval fish assemblages in the eastern central Atlantic. *Deep Sea Res. Part I: Oceanogr. Res. Pap.* **168**, 103446 (2021).
71. FAO. *The State of Mediterranean and Black Sea Fisheries 2020* (FAO, Rome, Italy, 2020).
72. Bertrand, A. et al. Oxygen: a fundamental property regulating pelagic ecosystem structure in the coastal southeastern tropical Pacific. *PLoS ONE* **6**, e29558 (2011).
73. Somarakis, S. et al. Daily egg production of anchovy in European waters. *ICES J. Mar. Sci.* **61**, 944–958 (2004).
74. Somarakis, S. & Nikolioudakis, N. Oceanographic habitat, growth and mortality of larval anchovy (Engraulis encrasicolus) in the northern Aegean Sea (eastern Mediterranean). *Mar. Biol.* **152**, 1143–1158 (2007).
75. Fernández-Corredor, E., Albo-Puigserver, M., Pennino, M. G., Bellido, J. M. & Coll, M. Influence of environmental factors on different life stages of European anchovy (Engraulis encrasicolus) and European sardine (Sardina pilchardus) from the Mediterranean Sea: a literature review. *Region. Stud. Mar. Sci.* **41**, 101606 (2021).
76. Marriner, N., Kaniewski, D., Pourkerman, M. & Devillers, B. Anthropocene tipping point reverses long-term Holocene cooling of the Mediterranean Sea: a meta-analysis of the basin's Sea Surface Temperature records. *Earth-Sci. Rev.* **227**, 103986 (2022).
77. Kuhnt, T., Schmiedl, G., Ehrmann, W., Hamann, Y. & Andersen, N. Stable isotopic composition of Holocene benthic foraminifers from the Eastern Mediterranean Sea: past changes in productivity and deep water oxygenation. *Palaeogeogr. Palaeoclimatol. Palaeoecol.* **268**, 106–115 (2008).
78. Agiadi, K. et al. Palaeontological evidence for community-level decrease in mesopelagic fish size during Pleistocene climate warming in the eastern Mediterranean. *Proc. R. Soc. B: Biol. Sci.* **290**, 20221994 (2023).
79. Elder, K. L., Jones, G. A. & Bolz, G. Distribution of otoliths in surficial sediments of the US Atlantic continental shelf and slope and potential for reconstructing Holocene fish stocks. *Paleoceanography* **11**, 359–367 (1996).
80. Lin, C.-H., Girone, A. & Nolf, D. Fish otolith assemblages from Recent NE Atlantic sea bottoms: a comparative study of palaeoecology. *Palaeogeogr. Palaeoclimatol. Palaeoecol.* **446**, 98–107 (2016).
81. Lin, C.-H., Chiang, Y.-P., Tuset, V. M., Lombarte, A. & Girone, A. Late quaternary to recent diversity of fish otoliths from the Red Sea, central Mediterranean, and NE Atlantic sea bottoms. *Geobios* **51**, 335–358 (2018).
82. Cartes, J. E. et al. Recent reconstruction of deep-water macrofaunal communities recorded in Continental Margin sediments in the Balearic Basin. *Deep Sea Res. Part I Oceanogr. Res. Pap.* **125**, 52–64 (2017).
83. Lin, C.-H., Taviani, M., Angeletti, L., Girone, A. & Nolf, D. Fish otoliths in superficial sediments of the Mediterranean Sea. *Palaeogeogr. Palaeoclimatol. Palaeoecol.* **471**, 134–143 (2017).
84. Pauly, D. et al. The biology of mesopelagic fishes and their catches (1950–2018) by commercial and experimental Fisheries. *J. Mar. Sci. Eng.* **9**, 1057 (2021).
85. Somarakis, S., Isari, S. & Machias, A. Larval fish assemblages in coastal waters of central Greece: reflections of topographic and oceanographic heterogeneity. *Sci. Mar.* **75**, 605–618 (2011).
86. Klevjer, T. A. et al. Large scale patterns in vertical distribution and behaviour of mesopelagic scattering layers. *Sci. Rep.* **6**, 19873 (2016).
87. Gersonde, R. The expedition of the research vessel "Sonne" to the subpolar North Pacific and the Bering Sea in 2009 (SO202-INOPEX). *Berichte zur Polar-und Meeresforschung=Reports on Polar and Marine Research*. Vol. 643, 323p (Alfred Wegener Institute for Polar and Marine Research, Bremerhaven, 2012).
88. Pross, J. et al. Eastern Mediterranean Paleoclimate and Ecosystems during the Rise of Early Civilizations, Cruise No. M144, December 27, 2017–January 18, 2018, Heraklion (Greece)–Catania (Italy). *METEOR-Berichte* (Gutachterpanel Forschungsschiffe, Bonn, 2021).
89. Koutsodendris, A. et al. Societal changes in Ancient Greece impacted terrestrial and marine environments. *Commun. Earth Environ.* **6**, 25 (2025).
90. Volkman, J. K., Barrerr, S. M., Blackburn, S. I. & Sikes, E. L. Alkenones in Gephyrocapsa oceanica: Implications for studies of paleoclimate. *Geochim. Cosmochim. Acta* **59**, 513–520 (1995).
91. Parisi-Baradad, V. et al. Automated taxon identification of teleost fishes using an otolith online database—AFORO. *Fish. Res.* **105**, 13–20 (2010).
92. Lombarte, A. et al. A web-based environment for shape analysis of fish otoliths. The AFORO database. *Sci. Mar.* **70**, 147–152 (2006).
93. Tuset, V. M., Lombarte, A. & Assis, C. A. Otolith atlas for the western Mediterranean, north and central eastern Atlantic. *Sci. Mar.* **72**, 7–198 (2008).
94. Agiadi, K. et al. The taphonomic clock in fish otoliths. *Paleobiology* **48**, 154–170 (2022).
95. Herguera, J. Last glacial paleoproductivity patterns in the eastern equatorial Pacific: benthic foraminifera records. *Mar. Micropaleontol.* **40**, 259–275 (2000).
96. R. Schlitzer. Ocean Data View, https://odv.awi.de (2023).
97. Zachariasse, W., Jorissen, F., Perissoratis, C. E., Rohling, E. & Tsapralis, V. In *Proceedings of the 5th Hellenic Symposium on Oceanography and Fisheries*, *Kavalla, Greece*. 15–18 (National centre for marine research, 1997).

Acknowledgements

We thank the captain and crew of the German R/V Meteor and the researchers as part of cruise M144 for supporting the sampling of this study. The Greek authorities are thanked for permitting research to be carried out in their territorial waters. We also thank Antoni Lombarte for his help on otolith taxonomy. We are grateful to Carla Rubio Gonçalves, Marta Bono García, and Lorenz Williams for laboratory assistance. Cruise M144 was supported by the Bundesministerium für Bildung und Forschung (BMBF) and the Deutsche Forschungsgemeinschaft (DFG), including J.P., A.B., O.F., and D. Nürnberg. RDN was supported by NSF-EAGER (1821140). A.V.S. acknowledges support from NSF-OCE1923998. S.P. acknowledges financial support from the FPI scholarship (BES-2017-080730) awarded by the Spanish Ministry of Economy and Competitiveness. This work contributes to the ICTA-UAB "María de Maeztu" program for Units of Excellence of the Spanish Ministry of Science and Innovation (MDM-2015-0552-16-2; CEX2019-000940-M). Further funding was received by MINECO PID2020-113526RB-I00, the Generalitat de Catalunya MERS (#2021 SGR-00640) and Horizon Europe (Grant Agreement ID: 101158830).

Author contributions

Conceptualization: S.P., R.D.N., P.Z. Methodology: S.P., A.V.S., C.H.L., R.D.N., O.F., J.P., S.K.-B., A.B., A.K., H.J. Investigation: S.P., R.D.N., O.F. Visualization: S.P. Supervision: R.D.N., P.Z. Writing—original draft: S.P.,

R.D.N. Writing—review & editing: S.P., R.D.N., P.Z., H.J., C.H.L., E.G., A.V.S., S.K.-B., O.F., A.B., A.K., J.P.

Competing interests
The authors declare no competing interests.

Additional information
Supplementary information The online version contains supplementary material available at https://doi.org/10.1038/s43247-025-02568-8.

Correspondence and requests for materials should be addressed to Sven Pallacks.

Peer review information *Communications Earth and Environment* thanks Konstantina Agiadi, Leticia Maria Cavole, and the other anonymous reviewer(s) for their contribution to the peer review of this work. Primary handling editors: Ilka Peeken, Carolina Ortiz Guerrero and Mengjie Wang. [A peer review file is available].